Miniworkshop on Diffraction and Ultraperipheral Collisions

Děčín 2018

J. Čepila

May 2, 2018

Contents

1 The scattering amplitude for vector meson production **2**

2 The wave function **3**
2.1 Gaussian models . . . 4
2.1.1 DGKP or Gauss-LC model . . . 5
2.1.2 Boosted Gaussian model . . . 6
2.2 non-Gaussian model . . . 7
2.2.1 Quarkonia potentials . . . 14

3 The dipole cross-section **16**
3.1 Balitsky-Kovchegov evolution equation . . . 17
3.1.1 MV initial conditions . . . 18
3.2 GBW . . . 19
3.3 KST . . . 19
3.4 IIM or CGC . . . 20
3.5 IP-sat or b-Sat or BGBK . . . 20
3.6 b-CGC . . . 21

1 The scattering amplitude for vector meson production

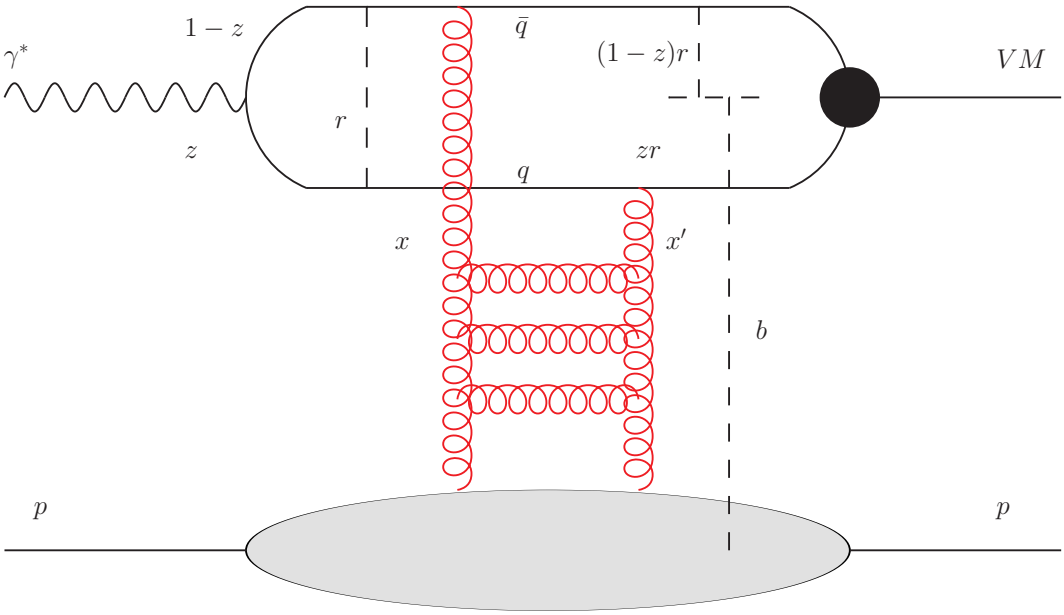

Figure 1: Interaction scheme of the vector meson production

The amplitude for production of a vector meson V is given by [1, 2, 3]

$$\mathcal{A}_{T,L}^{\gamma^* p \to Vp}(x_{Bj}, Q, \Delta) = i \int \mathrm{d}^2 r \int_0^1 \frac{\mathrm{d}z}{4\pi} \int \mathrm{d}^2 b \, \Psi_M^* \Psi_{\gamma^*} \Big|_{T,L} e^{-i(\vec{b}-(1-z)\vec{r})\Delta} \frac{\mathrm{d}\sigma_{q\bar{q}}}{\mathrm{d}^2 b}, \tag{1}$$

where $\Psi_M^* \Psi_{\gamma^*}|_{T,L}$ is an overlap of a virtual photon and vector meson wave function, $\Delta = \sqrt{-t}$ denotes the transverse momentum lost by the outgoing proton, $\vec{r}$ is the transverse dipole size, $\vec{b}$ is the impact parameter of the dipole(transverse distance from the center of the proton to the center of mass of the dipole) and z is a part of photon momenta carried by one of the quarks from the dipole,M_V is the mass of the vector meson, Q is the scale of the incoming photon, W is the energy of a photon and a hadron and Bjorken-x of produced meson is

$$x_{Bj} = \frac{Q^2 + M_V^2}{W^2 + Q^2}. \tag{2}$$

The elastic diffractive differential cross-section can be written as

$$\frac{\mathrm{d}\sigma_{T,L}^{\gamma^* p \to Vp}}{\mathrm{d}|t|} = \frac{1}{16\pi} \left| \mathcal{A}_{T,L}^{\gamma^* p \to Vp} \right|^2 \tag{3}$$

2 The wave function

The overlap of a virtual photon and vector meson wave function is defined as

$$\begin{aligned}\Psi_V^*\Psi_{\gamma^*}\Big|_T &= \frac{1}{2}\sum_{h,\bar{h}}\Psi^*_{h\bar{h}\lambda=+1}\Big|_V\Psi_{h\bar{h}\lambda=+1}\Big|_{\gamma^*}+\Psi^*_{h\bar{h}\lambda=-1}\Big|_V\Psi_{h\bar{h}\lambda=-1}\Big|_{\gamma^*}\\ \Psi_V^*\Psi_{\gamma^*}\Big|_L &= \sum_{h,\bar{h}}\Psi^*_{h\bar{h}\lambda=0}\Big|_V\Psi_{h\bar{h}\lambda=0}\Big|_{\gamma^*}.\end{aligned} \tag{4}$$

where h and $\bar{h}$ denote helicities of quarks and antiquark and λ is a polarization of incoming photon.

The photon wave function was calculated in perturbative QED[4, 5] from a $\gamma\to f\bar{f}$ vertex.

$$\begin{aligned}\Psi_{h\bar{h}\lambda=0}\Big|_{\gamma^*}(r,z,Q) &= e_f\delta_{f\bar{f}}e\sqrt{N_c}\delta_{h,-\bar{h}}2Qz(1-z)\frac{K_0(\epsilon r)}{2\pi} \qquad (5)\\ \Psi_{h\bar{h}\lambda=\pm1}\Big|_{\gamma^*}(r,z,Q) &= \pm e_f\delta_{f\bar{f}}e\sqrt{2N_c}\left(ie^{\pm i\theta_r}\left(z\delta_{h,\pm1}\delta_{\bar{h},\mp1}-(1-z)\delta_{h,\mp1}\delta_{\bar{h},\pm1}\right)\partial_r+m_f\delta_{h,\pm1}\delta_{\bar{h},\pm1}\right)\frac{K_0(\epsilon r)}{2\pi},\end{aligned}$$

where $e=\sqrt{4\pi\alpha_{em}}$, h, θ_r is the azimuthal angle between the vector $\vec{r}$ and the x-axis in the transverse plane, $\epsilon^2=z(1-z)Q^2+m_f^2$, $N_c=3$ is the number of colors, $e_f\delta_{f\bar{f}}$ and m_f are the fractional charge and effective mass of the quark respectively. The partial derivative of the modified Bessel function K_0 with respect to r can be done using the equation $\partial_r K_0(\epsilon r)=-\epsilon K_1(\epsilon r)$.

The vector meson wave function is modelled with the presumption that vector meson is predominantly a quark-antiquark state and the spin and polarization structure is the same as in the photon case [1]

$$\begin{aligned}\Psi_{h\bar{h}\lambda=0}\Big|_V(r,z,Q) &= \sqrt{N_c}\delta_{h,-\bar{h}}\left(M_V+\delta\frac{m_f^2-\nabla_r^2}{M_Vz(1-z)}\right)\Phi_L(r,z) \qquad (6)\\ \Psi_{h\bar{h}\lambda=\pm1}\Big|_V(r,z,Q) &= \pm\sqrt{2N_c}\frac{1}{z(1-z)}\left(ie^{\pm i\theta_r}\left(z\delta_{h,\pm1}\delta_{\bar{h},\mp1}-(1-z)\delta_{h,\mp1}\delta_{\bar{h},\pm1}\right)\partial_r+m_f\delta_{h,\pm1}\delta_{\bar{h},\pm1}\right)\Phi_T(r,z),\end{aligned}$$

where $\nabla_r^2=\frac{1}{r}\partial_r+\partial_r^2$ and δ is a switch enables to include the non-local part of the wave function introduced in [6, 7].

The overlap between photon and vector meson wave function is

$$\begin{aligned}\Psi_V^*\Psi_{\gamma^*}\Big|_T &= e_f\delta_{f\bar{f}}e\frac{N_c}{\pi z(1-z)}\left(m_f^2K_0(\epsilon r)\Phi_T(r,z)-(z^2+(1-z)^2)\epsilon K_1(\epsilon r)\partial_r\Phi_T(r,z)\right)\\ \Psi_V^*\Psi_{\gamma^*}\Big|_L &= e_f\delta_{f\bar{f}}e\frac{N_c}{\pi}2Qz(1-z)K_0(\epsilon r)\left(M_V\Phi_L(r,z)+\delta\frac{m_f^2-\nabla_r^2}{M_Vz(1-z)}\Phi_L(r,z)\right),\end{aligned} \tag{7}$$

where $e_f\delta_{f\bar{f}}$ is an effective charge that corresponds to the choice of the vector meson. It can be calculated for arbitrary meson from it's quark wave function by substituting charge for each quark-antiquark pair, e.g.

$$\rho=\frac{u\bar{u}-d\bar{d}}{\sqrt{2}}\Rightarrow e_\rho\delta_{f\bar{f}}=\frac{\frac{2}{3}-(-\frac{1}{3})}{\sqrt{2}}=\frac{1}{\sqrt{2}}\qquad J/\Psi=c\bar{c}\Rightarrow e_{J/\Psi}\delta_{f\bar{f}}=\frac{2}{3}. \tag{8}$$

The scalar part $\Phi_{T,L}$ of the vector meson wave function is model dependent. In the photon case the scalar part is given by modified Bessel functions (kind of a point object), whereas for the vector mesons the hadron at rest is more complicated object (kind of a sphere).

2.1 Gaussian models

These types of parametrization assume that transverse part of the vector meson in the rest frame can be approximated by a Gaussian in the transverse plane. It needs to specify two parameters - a width of a Gaussian R and a normalization of the scalar part N.

Normalization condition for the vector meson wave function comes from the fact, that the vector meson is composed solely of the quark-antiquark pair from the dipole. Therefore, no contribution from gluons and sea quarks is considered and

$$1 = \sum_{h,\bar{h}} \int \mathrm{d}^2 r \int_0^1 \frac{\mathrm{d}z}{4\pi} |\Psi^V_{h\bar{h}\lambda}(r,z,Q)|^2 \tag{9}$$

This can be transformed into the normalization of the scalar parts [1]

$$\begin{aligned} 1 &= \frac{N_c}{2\pi} \int_0^1 \frac{\mathrm{d}z}{z^2(1-z)^2} \int \mathrm{d}^2 r \left(m_f^2 \Phi_T^2(r,z) + (z^2 + (1-z)^2)(\partial_r \Phi_T(r,z))^2 \right) \\ 1 &= \frac{N_c}{2\pi} \int_0^1 \mathrm{d}z \int \mathrm{d}^2 r \left(M_V \Phi_L(r,z) + \delta \frac{m_f^2 - \nabla_r^2}{M_V z(1-z)} \Phi_L(r,z) \right)^2 . \end{aligned} \tag{10}$$

Another constraint on the vector meson wave functions is obtained from the decay width. It is assumed that the perturbative decay width of $\bar{q}q \to \gamma^* \to l^+ l^-$ is factorized from the vector meson wave function. The electromagnetic current is then

$$\begin{aligned} f_{V,T} &= e_f \frac{N_c}{2\pi M_V} \int_0^1 \frac{\mathrm{d}z}{z^2(1-z)^2} \left(m_f^2 - (z^2 + (1-z)^2)\nabla_r^2 \right) \Phi_T(r=0,z) \\ f_{V,L} &= e_f \frac{N_c}{\pi} \int_0^1 \mathrm{d}z \left(M_V + \delta \frac{m_f^2 - \nabla_r^2}{M_V z(1-z)} \right) \Phi_L(r=0,z). \end{aligned} \tag{11}$$

The coupling of the electromagnetic current to the vector meson is obtained from the measured electronic decay width as

$$\Gamma_{M \to e^+ e^-} = \frac{4\pi \alpha_{em}^2 f_V^2}{3 M_V}, \tag{12}$$

where the value of f_V comes from the measurement. It is presumed that $f_V = f_{V,L} = f_{V,T}$, however, some models predict different values of $f_{V,T}$ and $f_{V,L}$. In this case, the longitudinal part is preferably set to be equal to measured value [1].

Meson	$\Gamma_M[keV]$	$f_V[GeV]$
J/Ψ	5.547	0.2775
$\Psi(2S)$	2.351	0.1971
ρ	6.9762	0.1557
$\Upsilon(1S)$	1.2857	0.2335
$\Upsilon(2S)$	0.6108	0.16567

Table 1: Table of electromagnetic currents and decay widths of various vector mesons [8]

For excited states, one additional parameter means that we need one additional normalization conditions. It is, therefore, anticipated that 1S and 2S wave functions are orthogonal

$$0 = \frac{N_c}{2\pi}\int_0^1 \frac{\mathrm{d}z}{z^2(1-z)^2}\int \mathrm{d}^2r\left(m_f^2\Phi_T^{1S}(r,z)\Phi_T^{2S}(r,z) + (z^2+(1-z)^2)\partial_r\Phi_T^{1S}(r,z)\partial_r\Phi_T^{2S}(r,z)\right). \tag{13}$$

2.1.1 DGKP or Gauss-LC model

The Gauss-LC model [4] assumes that the longitudinal momentum fraction z fluctuates independently of the quark transverse momentum $\vec{k}$ (conjugate variable to $\vec{r}$). This model assumes $\delta = 0$.

$$\begin{aligned}\Phi_T(r,z) &= N_T(z(1-z))^2 e^{-\frac{r^2}{2R_T^2}} \\ \Phi_L(r,z) &= N_L z(1-z) e^{-\frac{r^2}{2R_L^2}}\end{aligned} \tag{14}$$

Meson	$\hat{e}_f$	$M_V[GeV]$	$m_f[GeV]$	N_T	$R_T^2[GeV^{-2}]$	N_L	$R_L^2[GeV^{-2}]$
J/Ψ	2/3	3.097	1.4	1.23	6.5	0.83	3.0
ρ	$1/\sqrt{2}$	0.776	0.14	4.47	21.9	1.79	10.4
$\Upsilon(1S)$	1/3	9.46	4.2	0.78	1.91	0.78	1.91

Table 2: Vector meson wave function parameters for the Gauss-LC static part from [1, 9]

.

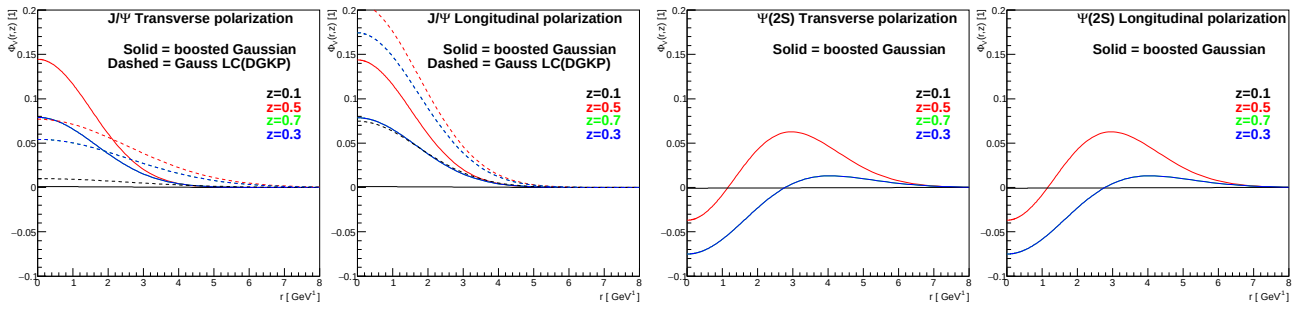

Figure 2: Scalar part of the J/Ψ and $\Psi(2S)$ wave function. Compare to [2].

2.1.2 Boosted Gaussian model

The boosted Gaussian model [6, 7, 10, 11] assumes that the fluctuation of the quark three-momentum $\vec{p}$ in the rest frame of the meson can be written in a boost-invariant form $p^2 = (k^2 + m_f^2)/(4z(1-z)) - m_f^2$. Therefore, supplying a scalar spatial part in the rest frame allows to boost it to proper frame. This model has proper short distance limit and assumes $\delta = 1$. If we use the Gaussian form of the rest frame meson wave function (quadratic potential in Schrodinger equation) we get

$$\Phi_{T,L}(r,z) = N_{T,L} z(1-z) e^{-\frac{m_f^2 R^2}{8z(1-z)} - \frac{2z(1-z)r^2}{R^2} + \frac{m_f^2 R^2}{2}} \tag{15}$$

Meson	$\hat{e}_f$	$M_V[GeV]$	$m_f[GeV]$	N_T	N_L	$R^2[GeV^{-2}]$
J/Ψ	$2/3$	3.097	1.4	0.578	0.575	2.3
ρ	$1/\sqrt{2}$	0.776	0.14	0.911	0.853	12.9
$\Upsilon(1S)$	$1/3$	9.46	4.2	0.481	0.480	0.57

Table 3: Table of vector meson wave function parameters for the boosted Gaussian static part from [1, 12]

For the first excited state 2S, the scalar wave function has the form

$$\Phi_{T,L}(r,z) = N_{T,L} z(1-z) e^{-\frac{m_f^2 R^2}{8z(1-z)} - \frac{2z(1-z)r^2}{R^2} + \frac{m_f^2 R^2}{2}} \times \left(1 + \alpha_{2S}\left(2 + \frac{m_f^2 R^2}{4z(1-z)} - \frac{4z(1-z)r^2}{R^2} - m_f^2 R^2\right)\right) \tag{16}$$

Meson	$\hat{e}_f$	$M_V[GeV]$	$m_f[GeV]$	N_T	N_L	$R^2[GeV^{-2}]$	$\alpha_{2S}[1]$
$\Psi(2S)$	$2/3$	3.686	1.4	0.67	0.67	3.72	-0.61
$\Upsilon(2S)$	$1/3$	10.023	4.2	0.624	0.624	0.831	-0.555

Table 4: Table of vector meson wave function parameters for the boosted Gaussian static part from [2, 13]

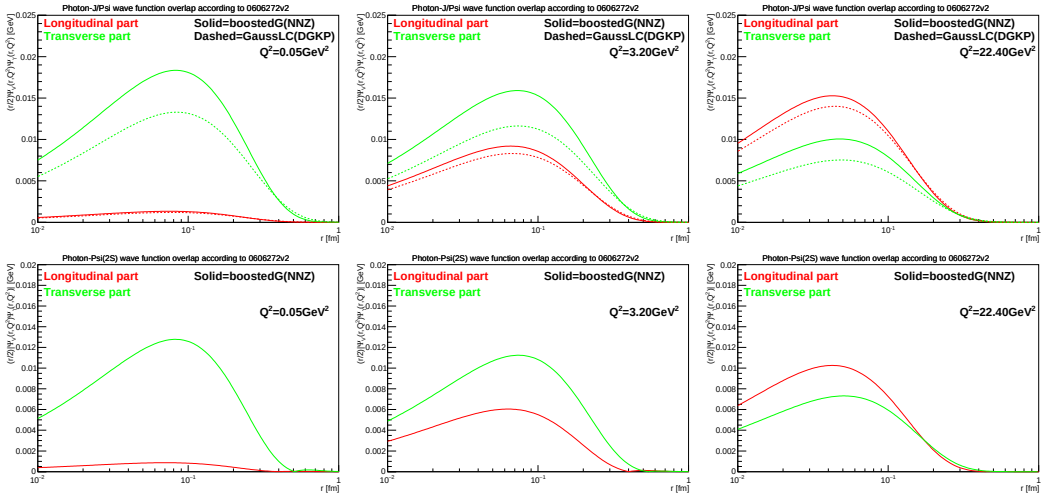

Figure 3: Overlap of photon-J/Ψ and photon-$\Psi(2S)$ wave functions for three values of Q^2. Compare to [1].

2.2 non-Gaussian model

The boosted non-Gaussian model (also called NNPZ) [6, 7, 11, 14] assumes as in Gaussian version that the fluctuation of the quark three-momentum $\vec{p}$ in the rest frame of the meson can be written in a boost-invariant form. But rather than guessing the rest frame form of a wave function, it supplies the solution of the Schrodinger equation for realistic potential. The spatial part of the $q\bar{q}$ wave function satisfies the Schrodinger equation [14]

$$\left(-\frac{\Delta}{2\mu}+V(r)\right)\Psi_{nlm}(\vec{r})=E_{nl}\Psi_{nlm}(\vec{r}), \tag{17}$$

$$\mu=\frac{m_q m_{\bar{q}}}{m_q+m_{\bar{q}}}=\frac{m_q}{2}, \tag{18}$$

where μ is the reduced mass of the $q\bar{q}$ pair and

$$\Delta=\sum_{i=1}^{3}\frac{\partial^2}{\partial x_i^2}=\frac{1}{r^2}\frac{\partial}{\partial r}\left(r^2\frac{\partial}{\partial r}\right)+\frac{1}{r^2\sin\theta}\frac{\partial}{\partial\theta}\left(\sin\theta\frac{\partial}{\partial\theta}\right)+\frac{1}{r^2\sin^2\theta}\frac{\partial^2}{\partial\varphi^2}. \tag{19}$$

If we use the standard factorized form of the wave function to radial and angular part

$$\Psi_{nlm}(\vec{r})=\psi_{nl}(r)\times Y_{lm}(\theta,\varphi) \tag{20}$$

the Schrodinger equation can be separated to two equations

$$\begin{aligned}\frac{\partial}{\partial r}\left(r^2\frac{\partial\psi(r)}{\partial r}\right)+m_q(E-V(r))r^2\psi(r) &= l(l+1)\psi(r)\\ \frac{1}{\sin\theta}\frac{\partial}{\partial\theta}\left(\sin\theta\frac{\partial Y(\theta,\varphi)}{\partial\theta}\right)+\frac{1}{\sin^2\theta}\frac{\partial^2 Y(\theta,\varphi)}{\partial\varphi^2} &= -l(l+1)Y(\theta,\varphi)\end{aligned} \tag{21}$$

with $l=0$ for 1S,2S states and $l=1$ for 1P,2P etc. If there is no spin rotation, the solution of angular equation provides constant factor, that is absorbed into the normalization. For the solution of the radial equation, the potentials from Section 2.2.1 were used
Now, we can use the formula

$$\frac{1}{r^2}\frac{\partial}{\partial r}\left(r^2\frac{\partial\psi(r)}{\partial r}\right)=\frac{1}{r}\frac{\partial^2}{\partial r^2}\left(r\psi(r)\right) \tag{22}$$

to rewrite the radial Schrodinger equation to

$$\frac{1}{r}\frac{\partial^2}{\partial r^2}\left(r\psi(r)\right)+m_q(E-V(r))\psi(r)=\frac{l(l+1)}{r^2}\psi(r). \tag{23}$$

If we use a substitution $u(r)=r\psi(r)$ we have

$$\frac{\partial^2 u(r)}{\partial r^2}+m_q(E-V(r))u(r)=\frac{l(l+1)}{r^2}u(r). \tag{24}$$

This can be written in the final form

$$\frac{\partial^2 u(r)}{\partial r^2}=(V_{eff}(r)-\epsilon)u(r)\qquad V_{eff}(r)=m_qV(r)+\frac{l(l+1)}{r^2}\qquad \epsilon=m_qE. \tag{25}$$

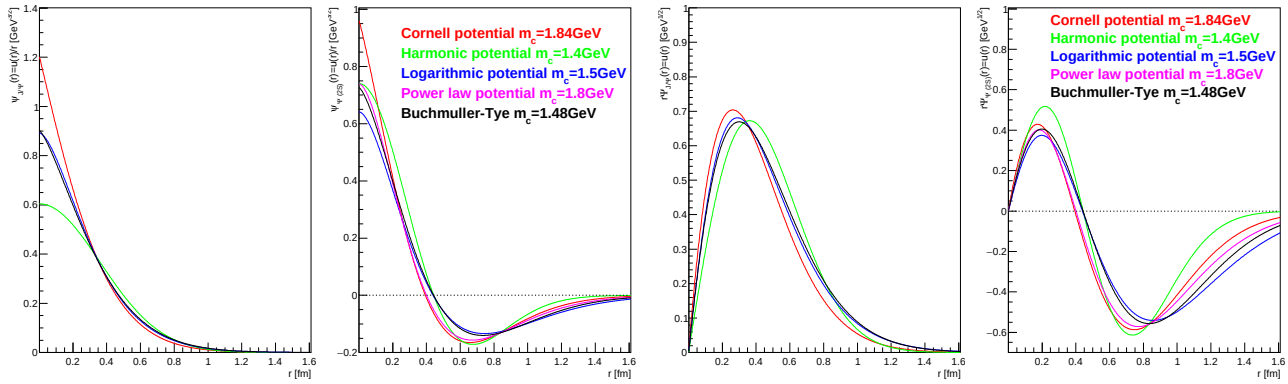

Figure 4: Normalized reduced and non-reduced solution of the Schrodinger equation. Compare [14] Fig. 4.

This equation can be solved using e.g. Runge-Kutta method with initial conditions[15] $r = r_{min}, u(r_{min}) = r_{min}^{l+1}, u'(r_{min}) = (l+1)r_{min}^{l}$ or Numerov method with initial conditions $r = r_{min}, u(r_{min}) = r_{min}^{l+1}, u(r_{min+1}) = r_{min+1}^{l+1}$. Both methods lead to almost the same results, so we used the latter one, since it is faster. The normalization of the solution is that the following relation holds

$$\int_0^{+\infty} |u(r)|^2 \mathrm{d}r = 1 \tag{26}$$

and so, $u(r)$ has a dimension $\mathrm{GeV}^{\frac{1}{2}}$ and $\psi_{nl}(r)$ has a dimension $\mathrm{GeV}^{\frac{3}{2}}$. The solution can be tested by calculating overall normalization and mean values of the distribution. Results for these values are summarized in the following table

J/Ψ	$\epsilon[GeV^2]$	$\int \lvert u\rvert^2 \mathrm{d}r[1]$	$< 1/r > [GeV]$	$< 1/r^2 > [GeV^2]$	$< r^2 > [GeV^{-2}]$
Cornell	0.4738	0.6936	0.8085	1.171	3.6345
Harmonic	0.891	2.738	0.6149	0.5936	5.051
Logarithmic	0.1008	1.257	0.7235	0.893	4.364
Buchmuller-Tye	0.185	1.2286	0.707	0.866	4.58

Table 5: Table of testing parameters for the solution of the Schrodinger equation for J/Ψ.

$\Psi(2S)$	$\epsilon[GeV^2]$	$\int \lvert u\rvert^2 \mathrm{d}r[1]$	$< 1/r > [GeV]$	$< 1/r^2 > [GeV^2]$	$< r^2 > [GeV^{-2}]$
Cornell	1.560	1.088	0.4628	0.619	14.84
Harmonic	2.079	1.825	0.5124	0.593	11.78
Logarithmic	0.985	2.432	0.3721	0.386	20.76
Buchmuller-Tye	1.077	1.896	0.4069	0.458	18.50

Table 6: Table of testing parameters for the solution of the Schrodinger equation for $\Psi(2S)$.

Since the solution of the Schrodinger equation $u(r)$ is normalized the actual wave function $\psi(r)$ is then

normalized as follows

$$\psi(r) = \frac{u(r)}{r}\,[\mathrm{GeV}^{\frac{3}{2}}] \qquad \int_0^{+\infty} |u(r)|^2 \mathrm{d}r = 1 \;\Rightarrow\; \int |\psi(r)|^2 \mathrm{d}^3 r = 4\pi. \tag{27}$$

In order to obtain normalized wave function, we have to re-normalize it according to previous formula with

$$\psi(r) = \frac{1}{\sqrt{4\pi}}\psi(r). \tag{28}$$

This normalized solution has to be now Fourier transformed (notation according to [16]) to momentum space using following definition of Fourier transformation

$$\psi(y) = \frac{1}{(2\pi)^{\frac{n}{2}}} \int e^{i\vec{x}\vec{y}}\psi(x)\mathrm{d}^n x \qquad \psi(x) = \frac{1}{(2\pi)^{\frac{n}{2}}} \int e^{-i\vec{x}\vec{y}}\psi(y)\mathrm{d}^n y \tag{29}$$

yielding

$$\psi(p) = \frac{1}{(2\pi)^{\frac{3}{2}}} \int \mathrm{d}^3 r\, e^{i\vec{p}\vec{r}}\psi(r) = \frac{1}{(2\pi)^{\frac{3}{2}}} \int_0^{+\infty} r^2 \mathrm{d}r\psi(r) \int_0^{2\pi} \mathrm{d}\phi \int_0^{\pi} \mathrm{d}\theta e^{ipr\cos\theta}\sin\theta. \tag{30}$$

We can use the integral definition of the Bessel function

$$J_{\frac{1}{2}}(t) = \frac{\sqrt{t}}{\sqrt{2\pi}} \int_0^{\pi} e^{it\cos\theta}\sin\theta \mathrm{d}\theta = \sqrt{\frac{2}{\pi t}}\sin(t) \tag{31}$$

to write

$$\psi(p) = \frac{2\pi}{(2\pi)^{\frac{3}{2}}} \int_0^{+\infty} r^2 \mathrm{d}r\psi(r) J_{\frac{1}{2}}(pr) \frac{\sqrt{2\pi}}{\sqrt{pr}} \tag{32}$$

and, consequently,

$$\psi(p) = \frac{2}{\sqrt{2\pi}p} \int_0^{+\infty} r\mathrm{d}r\psi(r)\sin(pr) \quad [\mathrm{GeV}^{-\frac{3}{2}}]. \tag{33}$$

The normalization is such that the integral in the Fourier transformation has to leave the normalization intact and following the fact that we started with the wave function normalized to 1 we have (see [17])

$$\int |\psi(p)|^2 \mathrm{d}^3 p = 1. \tag{34}$$

Now, the wave function in momentum space has to be boosted to proper frame. The procedure used in [14] was adapted. Note, that it differs from the one in [16] by a factor $\frac{1}{2}$ in the definition of unit phase space. We use the fact that invariant mass of the quark pair is the same in all frames and we can write it in terms of light-cone variables ([6, 14, 16]) as

$$M_{q\bar{q}} = (p_q + p_{\bar{q}})^2 = \frac{p_T^2 + m_q^2}{z(1-z)} \tag{35}$$

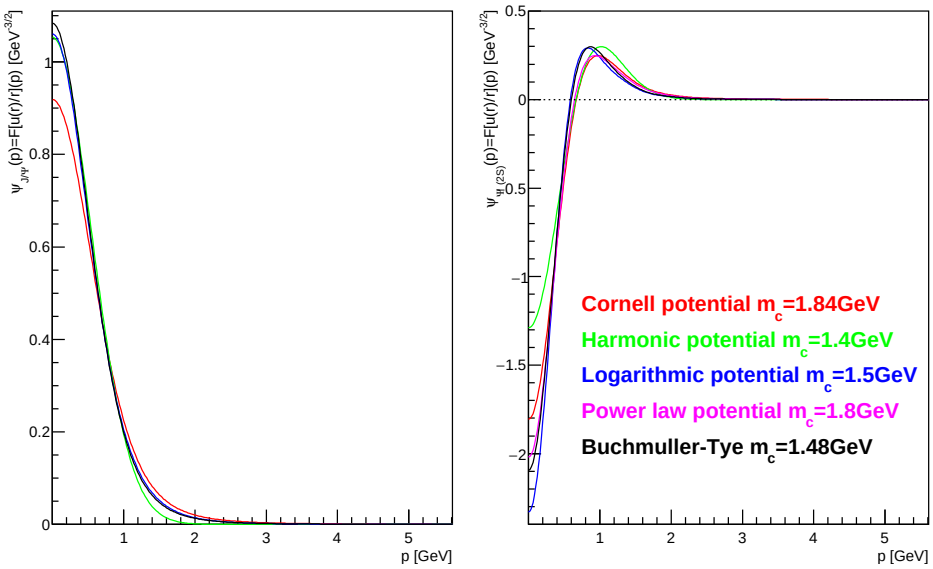

Figure 5: Fourier transformed wave function.

J/Ψ	$\int \|\psi\|^2 \mathrm{d}^3p[1]$	$< 1/p > [GeV^{-1}]$	$< 1/p^2 > [GeV^{-2}]$	$< p^2 > [GeV^2]$
Cornell	0.9999	1.825	5.409	0.673
Harmonic	0.9999	2.070	6.706	0.445
Logarithmic	0.9999	2.004	6.529	0.5497
Buchmuller-Tye	0.9999	2.044	6.757	0.523

Table 7: Table of testing parameters for the Fourier transform for J/Ψ.

$\Psi(2S)$	$\int \|\psi\|^2 \mathrm{d}^3p[1]$	$< 1/p > [GeV^{-1}]$	$< 1/p^2 > [GeV^{-2}]$	$< p^2 > [GeV^2]$
Cornell	0.9999	2.393	11.762	0.815
Harmonic	0.9999	1.725	6.692	1.039
Logarithmic	0.9999	2.931	16.98	0.560
Buchmuller-Tye	0.9999	2.646	14.333	0.647

Table 8: Table of testing parameters for the Fourier transform for $\Psi(2S)$.

assuming quarks are on shell and the same can be done in the rest frame of the quark pair as

$$M_{q\bar{q}} = (p_q + p_{\bar{q}})^2 = (2E)^2 = 4(p^2 + m_q^2) \tag{36}$$

since $\vec{p}_q = -\vec{p}_{\bar{q}}$. And so, following relations hold

$$4(p^2 + m_q^2) = \frac{p_T^2 + m_q^2}{z(1-z)} \qquad p^2 = \frac{p_T^2 + (1-2z)^2 m_q^2}{4z(1-z)} \qquad p_L^2 = \frac{(p_T^2 + m_q^2)(1-2z)^2}{4z(1-z)}. \tag{37}$$

The identification between wave functions in both frames is done using probability conservation per unit phase space

$$\mathrm{d}^3p|\psi(p)|^2 = \mathrm{d}^2p_T\mathrm{d}z|\psi(p_T,z)|^2. \tag{38}$$

We need to express d^3p in terms of light-cone variables. This can be done using

$$\mathrm{d}^3p = \mathrm{d}p_L\mathrm{d}^2p_T, \tag{39}$$

where

$$\mathrm{d}p_L = \frac{\sqrt{p_T^2 + m_q^2}}{4\sqrt{(z(1-z))^3}}\mathrm{d}z \tag{40}$$

and from the correspondence equation we have

$$\frac{\sqrt{p_T^2 + m_q^2}}{4\sqrt{(z(1-z))^3}}\mathrm{d}z\mathrm{d}^2p_T|\psi(p)|^2 = \mathrm{d}^2p_T\mathrm{d}z|\psi(p_T,z)|^2 \tag{41}$$

and we can write the formula for the boosted wave function in $(z, \vec{p}_T)$ space as

$$\psi(p_T,z) = \psi\left(p = \sqrt{\frac{p_T^2 + (1-2z)^2 m_q^2}{4z(1-z)}}\right)\left(\frac{p_T^2 + m_q^2}{16(z(1-z))^3}\right)^{\frac{1}{4}} \qquad [\mathrm{GeV}^{-1}] \tag{42}$$

or

$$\psi(p_T,z) = \psi\left(p = \sqrt{\frac{p_T^2 + (1-2z)^2 m_q^2}{4z(1-z)}}\right)\sqrt{2}\left(\frac{(p^2 + m_q^2)^{\frac{3}{4}}}{(p_T^2 + m_q^2)^{\frac{1}{2}}}\right) \qquad [\mathrm{GeV}^{-1}]. \tag{43}$$

Following previous definition of the normalization and the Fourier transformation, this wave function has to be normalized according to

$$1 = \int |\psi(p)|^2\mathrm{d}^3p = \int |\psi(p_T,z)|^2\mathrm{d}^2p_T\mathrm{d}z = \int |\psi(p_T,z)|^2 2\pi p_T\mathrm{d}p_T\mathrm{d}z. \tag{44}$$

	Cornell	Harmonic	Logarithmic	Power law	Buchmuller-Tye
J/Ψ	1.0001	1.0000	1.0001		1.0001
$\Psi(2S)$	0.9998	0.9996	0.9997	0.9998	0.9997

Table 9: Table of normalizations of boosted wave functions in (p_T, z) space according to previous formula.

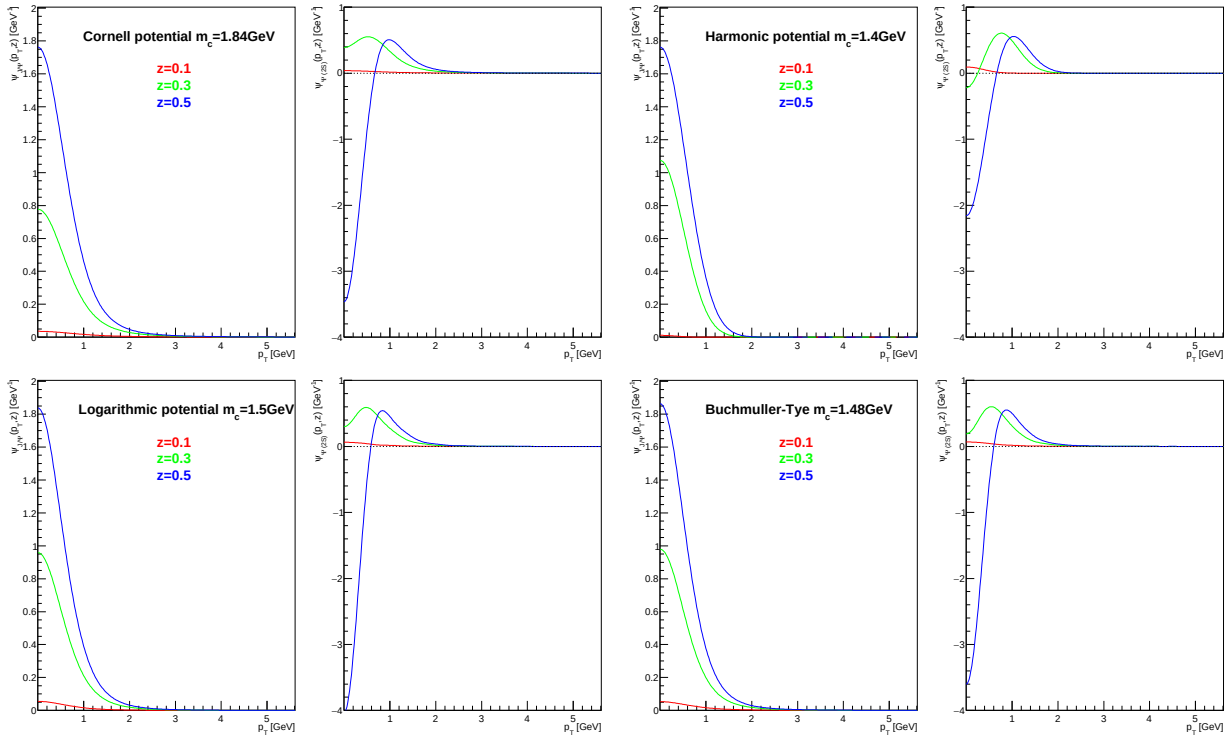

Figure 6: Boosted Fourier transformed wave function for fixed values of z.

Note, that the correspondence (38) in [16] has additional factor $\frac{1}{2}$.
The final form of the wave function is done by transforming the wave function from (p_T, z) space to (r, z) space using 2D Fourier transformation

$$\psi(r,z) = \int \frac{\mathrm{d}^2 p_T}{2\pi} e^{-i\vec{p}_T\vec{r}}\psi(p_T,z) = \int\limits_0^{+\infty} \frac{p_T \mathrm{d}p_T}{2\pi}\psi(p_T,z)\int\limits_0^{2\pi}\mathrm{d}\theta e^{-ipr\cos\theta} = \int\limits_0^{+\infty} p_T \mathrm{d}p_T \psi(p_T,z) J_0(p_T r). \quad (45)$$

The resulting wave function is then in GeV.
Following previous definitions of the normalization and the Fourier transformation, this wave function has to be normalized according to

$$1 = \int |\psi(p_T,z)|^2 \mathrm{d}^2 p_T \mathrm{d}z = \int |\psi(r,z)|^2 \mathrm{d}^2 r \mathrm{d}z = 2\pi \int |\psi(r,z)|^2 r \mathrm{d}r\mathrm{d}z. \quad (46)$$

	Cornell	Harmonic	Logarithmic	Power law	Buchmuller-Tye
J/Ψ	1.0001	1.0000	1.0001		1.0001
$\Psi(2S)$	0.9997	0.9996	0.9996	0.9997	0.9968

Table 10: Table of normalizations of backward Fourier transformed boosted wave functions in (r, z) space according to previous formula.

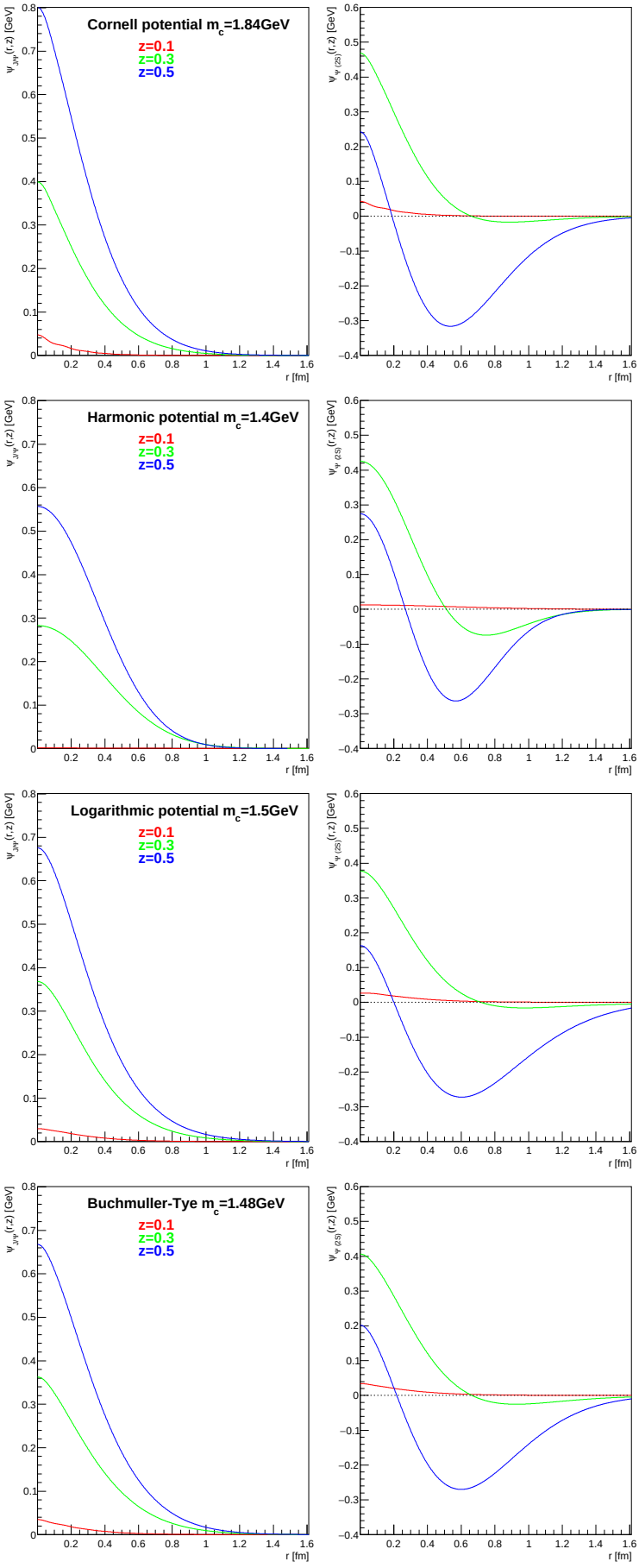

Figure 7: Backward Fourier transformed boosted wave function for fixed values of z. Compare [14] Fig. 5.

2.2.1 Quarkonia potentials

In order to calculate the radial part of the wave function of vector mesons, one needs to specify a potential between these two quarks. This potential is used for the solution of the Schrodinger equation in the rest frame of the pair.

Harmonic oscillator potential
Most common choice of the potential leads to the gaussian shape of the wave function. It is used in Gaussian models.

$$V(r) = \frac{1}{2} m_q \omega^2 r^2, \tag{47}$$

where

$$\omega = \frac{1}{2}(M_{2S} - M_{1S}) \tag{48}$$

which is 0.3GeV for J/Ψ and 0.28GeV for Υ. The mass of the quark is taken $m_c = 1.4$ GeV and $m_b = 4.2$GeV. Schrodinger equation with this potential has analytic solution in the form

$$u(r) = e^{-\frac{1}{4} m_q \omega r^2} \tag{49}$$

and mean square of the radius is $< r^2 >= \frac{2}{m_q \omega}$.

Cornell potential
The Cornell potential was published in [18, 19] and also used in [16, 14]

$$V(r) = -\frac{k}{r} + \frac{r}{a^2} \quad k = 0.52 \quad a = 2.34\text{GeV}^{-1} \tag{50}$$

with $m_c = 1.84$ GeV and $m_b = 5.17$ GeV.

Logarithmic potential
This potential is taken from [14] and it is motivated by potential in [20].

$$V(r) = -0.6635\text{GeV} + (0.733\text{GeV}) \log(r.1\text{GeV}) \tag{51}$$

with $m_c = 1.5$GeV and $m_b = 5$ GeV.

Power law potential
This potential is taken from [14] and it is motivated by potential in [21].

$$V(r) = -8.064\text{GeV} + (6.898\text{GeV})(r.1\text{GeV})^{0.1} \tag{52}$$

with $m_c = 1.8$GeV.

Buchmuller-Tye potential
This potential has a Coulomb like behaviour for small r and string-like behaiour at large r. It has similar structure like Cornell potential, but there are some corrections to the small r part. For details see [22]. This potential uses $m_c = 1.48$GeV and $m_b = 4.87$GeV.

$$V(r) = \frac{k}{r} - \frac{8\pi}{27} \frac{v(\lambda r)}{r} \qquad r \geq 0.01\text{fm} \tag{53}$$

$$V(r) = -\frac{16\pi}{25}\frac{1}{r\ln\left(\frac{1}{\lambda_{MS}^2 r^2}\right)}\left(1 + 2\left(\gamma_E + \frac{53}{75}\right)\frac{1}{\ln\left(\frac{1}{\lambda_{MS}^2 r^2}\right)} - \frac{462}{625}\frac{\ln\left(\ln\left(\frac{1}{\lambda_{MS}^2 r^2}\right)\right)}{\ln\left(\frac{1}{\lambda_{MS}^2 r^2}\right)}\right) \qquad r < 0.01\text{fm}$$

$$\Lambda_{MS} = 0.509\text{GeV} \qquad k = 0.153\text{GeV}^2 \qquad \lambda = 0.406\text{GeV} \qquad \gamma_E = 0.5772 \tag{54}$$

and the function $v(x)$ is interpolated from the table published in [22]

x	0	0.01	0.02	0.03	0.04	0.05	0.1	0.2	0.3	0.4	0.5	0.6	0.7
$v(x)$	0	0.249	0.3	0.339	0.37	0.397	0.499	0.624	0.707	0.766	0.811	0.845	0.872
x	0.8	0.9	1.0	1.1	1.2	1.3	1.4	1.5	1.6	1.7	1.8	1.9	2.0
$v(x)$	0.893	0.911	0.925	0.936	0.946	0.953	0.96	0.965	0.97	0.974	0.977	0.98	0.982

Table 11: Table of values of the function $v(x)$.

According to [22] the mean square of the radius has following values

$$< r^2_{J/\Psi} >= 0.1764 \qquad < r^2_{\Psi(2S)} >= 0.7225 \qquad < r^2_{\Upsilon} >= 0.0529 \qquad < r^2_{\Upsilon(2S)} >= 0.25 \tag{55}$$

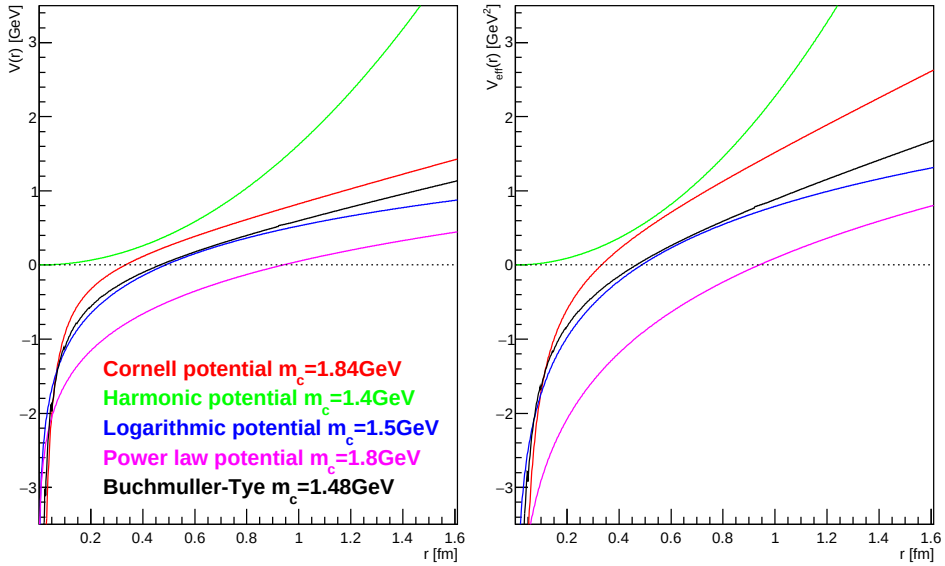

Figure 8: Left: Various potentials used for the calculation. Compare to Fig. 3 of [14]. Right: Effective potentials V_{eff} for $L = 0$ and c-quark.

3 The dipole cross-section

In general, the dipole cross-section $\sigma_{q\bar{q}}$ depends on the transverse separation of the dipole $\vec{r}$, on Bjorken variable x and on the impact parameter $\vec{b}$ of the dipole in the rest frame of the target. The dipole cross-section behave like $\sim r^2$ at small separations $r \to 0$. However, at large separations the dipole cross-section is presumed to be saturated in order to suppress contributions from very large dipoles(black disc limit). The differential dipole cross-section can be expressed via optical theorem as

$$\frac{\mathrm{d}\sigma_{q\bar{q}}}{\mathrm{d}^2 b} = 2N(x, r, b). \tag{56}$$

So, either we do provide a parametrization of this N (which is very complicated to do) or we try to reduce the complexity by using some ad-hoc factorization. Since most of the dipole cross-sections are independent of impact parameter b, one has to modify the formula for the scattering amplitude. Let's assume the transverse distribution of the gluonic density in the proton is T_p, then one can write

$$\frac{\mathrm{d}\sigma_{q\bar{q}}}{\mathrm{d}^2 b} = 2N(x, r, b) = \sigma_0 N(x, r) T_p(b) \tag{57}$$

so that one can integrate over impact parameter to have

$$\sigma_{q\bar{q}}(x, r) = \int \mathrm{d}^2 b \sigma_0 N(x, r) T_p(b) = \sigma_0 N(x, r), \tag{58}$$

The simplest form of the gluon profile function is a step function

$$T_p(b) = \frac{1}{\pi b_s^2} \Theta(b_s - b) \Rightarrow \int \mathrm{d}^2 b T_p(b) = 1, \tag{59}$$

where the parameter $b_s = 4$ GeV^{-1}[1] is a parameter fixed by the average square transverse radius of the proton $\langle b^2 \rangle = \frac{b_s^2}{2}$. Other possible profile function is a Gauss distribution

$$T_p(b) = \frac{1}{2\pi B} e^{-\frac{b^2}{2B}} \Rightarrow \int \mathrm{d}^2 b T_p(b) = 1 \tag{60}$$

where the parameter B is taken from the fit to experimental data. The value $B = 5.59$ GeV^{-2} is discussed in [23].

Other version of the transverse profile of the proton can be formulated from pion exchange model. It is based on the idea that proton has a hard core given by steep gaussian surrounded by soft pion cloud given by broad gaussian. Both gaussians are centered in the middle of the proton

$$T_p(b) = \frac{1}{4\pi B_h} e^{-\frac{b^2}{2B_h}} + \frac{1}{4\pi B_s} e^{-\frac{b^2}{2B_s}} \Rightarrow \int \mathrm{d}^2 b T_p(b) = 1 \tag{61}$$

The values of hard and soft width B_h and B_s has to be fitted to data. Our initial choice was $B_h = 0.25\mathrm{GeV}^{-2}$ and $B_s = 5.25\mathrm{GeV}^{-2}$.

Also, one can construct the proton profile function from individual gluons of gluonic clusters (hot spots). We take gaussian hot spots with fixed size $B_{hs} = 0.8\mathrm{GeV}^{-2}$ and put them at a position $\vec{b_i}$ generated from a gaussian distribution corresponding to a proton with the width $B_p = 4.7\mathrm{GeV}^{-2}$. The final formula reads [24]

$$T_p(b) = \frac{1}{N_{hs}} \sum_{i=1}^{N_{hs}} T_g(\vec{b} - \vec{b_i}) \qquad T_g(b) = \frac{1}{2\pi B_{hs}} e^{-\frac{b^2}{2B_{hs}}} \Rightarrow \int \mathrm{d}^2 b T_p(b) = 1, \tag{62}$$

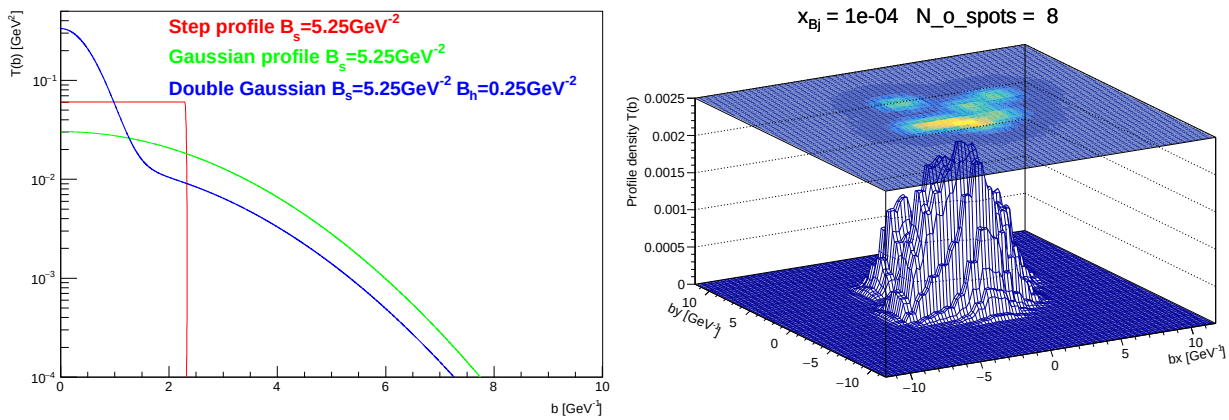

Figure 9: Shapes of the transverse profile of the proton using verious models. Right figure shows a profile generated from hot spots. Since the formula for scattering amplitude no longer depends on the magnitude of the impact parameter, we have to use 2D distribution in contrast to standard profile functions. Details see [24].

where the number of hot spots is an unknown functional parameter of the model. We took a formula very loosely motivated by PDF's [24]

$$N_{hs}(x) = 0.011x^{-0.58}(1 + 250\sqrt{x}), \tag{63}$$

where we presume that the number of hot spots will rise with decreasing Bjorken-x.

3.1 Balitsky-Kovchegov evolution equation

The BK equation describes the evolution in rapidity Y of the scattering amplitude $N(r, Y)$ for the scattering of a colour dipole of transverse size r with a target. During the evolution the dipole may split into two dipoles or two dipoles may recombine into one. This formulation is based on the work of [25, 26, 27] and study the equation without impact parameter dependance. The running coupling Balitsky–Kovchegov equation [28, 29] is

$$\frac{\partial N(r,Y)}{\partial Y} = \int d\vec{r}_1 K(\vec{r},\vec{r}_1,\vec{r}_2)\Big(N(r_1,Y) + N(r_2,Y) - N(r,Y) - N(r_1,Y)N(r_2,Y)\Big) \tag{64}$$

where $\vec{r}_2 = \vec{r} - \vec{r}_1$; $r = |\vec{r}|$ and similarly for r_1 and r_2. The kernel corresponding to the fixed coupling [26] is

$$K(\vec{r},\vec{r}_1,\vec{r}_2) = \frac{\alpha_s N_C}{2\pi^2}\frac{r^2}{r_1^2 r_2^2}, \tag{65}$$

with α_s fixed to some scale. The kernel incorporating the running of the coupling [27] is given by

$$K(\vec{r},\vec{r}_1,\vec{r}_2) = \frac{\alpha_s(r^2)N_C}{2\pi^2}\left(\frac{r^2}{r_1^2 r_2^2} + \frac{1}{r_1^2}\left(\frac{\alpha_s(r_1^2)}{\alpha_s(r_2^2)} - 1\right) + \frac{1}{r_2^2}\left(\frac{\alpha_s(r_2^2)}{\alpha_s(r_1^2)} - 1\right)\right), \tag{66}$$

with

$$\alpha_s(r^2) = \frac{4\pi}{(11 - \frac{2}{3}N_f)\ln\left(\frac{4C^2}{r^2\Lambda^2_{QCD}}\right)} \tag{67}$$

where N_f is the number of active flavours and C is a parameter to be fixed by comparing to data. Usually, one is forced to cut the growth of the coupling constant, not allowing $\alpha_s(r^2)$ to exceed some fixed value in the range 0.5-1. There are two approaches to set the Λ_{QCD}. In fixed number of flavours scheme, the value is set to $\Lambda_{QCD} = 0.241$MeV. In variable number of flavours scheme, each flavour has its Λ_{QCD} calculated from recurrent relation

$$\Lambda_{N_f-1} = m_f^{1-\frac{\beta_{N_f}}{\beta_{N_f-1}}} \Lambda_{N_f}^{\frac{\beta_{N_f}}{\beta_{N_f-1}}}, \tag{68}$$

where $\beta_{N_f} = (11N_c - 2N_f)/3$ and m_f is the mass of the quark of flavour f. As a starting point one can take measured $\alpha_s(r^2 = 4C^2/M_Z^2) = 0.1189$ for $n_f = 5$ at a scale of Z boson mass $M_Z = 91.187$GeV. This leads to the formula

$$\Lambda_5 = M_Z e^{-\frac{2\pi}{\alpha_s(r^2=4C^2/M_Z^2)\beta_5}}. \tag{69}$$

For variable scheme, if $r^2 < 4C^2/m_b^2$, one has to use the value of Λ_5 in the formula for $\alpha_s(r^2)$. If $4C^2/m_b^2 < r^2 < 4C^2/m_c^2$, one has to use the value of Λ_4 in the formula for $\alpha_s(r^2)$ and, finally, if $4C^2/m_c^2 < r^2$, one has to use the value of Λ_3 in the formula for $\alpha_s(r^2)$, since mass of light quarks are usually taken to be the same. The collinearly improved kernel [30] is given by

$$K(\vec{r},\vec{r}_1,\vec{r}_2) = \frac{\bar{\alpha}_s N_C}{2\pi^2}\left(\frac{r^2}{r_1^2 r_2^2}\left(\frac{r^2}{\min(r_1^2,r_2^2)}\right)^{\pm\bar{\alpha}_s A_1}\frac{J_1(2\sqrt{\bar{\alpha}_s|\ln(r_1^2/r^2)\ln(r_2^2/r^2)|})}{\sqrt{\bar{\alpha}_s|\ln(r_1^2/r^2)\ln(r_2^2/r^2)|}}\right), \tag{70}$$

with $A_1 = 11/12$, the positive sign refers to the situation where $r < \min(r_1, r_2)$ and $\bar{\alpha}_s = \alpha_s(\min(r^2, r_1^2, r_2^2))\frac{N_c}{\pi}$. The rcBK equation can be solved numerically using Runge–Kutta (RK) methods in parallel over a grid in r.

3.1.1 MV initial conditions

For the initial form of the dipole scattering amplitude the McLerran-Venugopalan model [31] can be used:

$$N(r, Y = 0) = 1 - \exp\left(-\frac{\left(r^2 Q_{s0}^2\right)^\gamma}{4}\ln\left(\frac{1}{r\Lambda_{QCD}} + e\right)\right) \tag{71}$$

with the values of the parameters Q_{s0}^2, C and γ taken from fit (e) in Table 1 of [27]. Note that in the fit the initial rapidity, $Y = 0$, is at $x_0 = 0.01$, where the relation between Y and x is $Y = \ln(x_0/x)$. Within this prescription rapidity $Y = 7$ corresponds to $x \approx 10^{-5}$; that is, to the smallest x measured at HERA for perturbative scales. The fit using $m_{uds} = 0.14$GeV, $m_c = 1.27$GeV and $m_b = 4.18$GeV yielded the following values for the parameters: $\sigma_0 = 32.895$mb, $Q_{s0}^2 = 0.165$ GeV^2, $\gamma = 1.135$ and $C = 2.52$. The fit was performed under the assumption that $\alpha_s(r^2)$ freezes for values of r larger than r_0 defined by $\alpha_s(r_0^2) = 0.7$. Fixed number of flavour scheme is usually used fixing Λ_{QCD} to 241 MeV and $N_f = 3$. A collinear version of MV initial conditions was published in [30]

$$N(r, Y = 0) = \left[1 - \exp\left(-\left[\frac{r^2 Q_{s0}^2}{4}\bar{\alpha}_s(r^2)\left(1 + \ln\left(\frac{\alpha_{sat}}{\bar{\alpha}_s(r^2)}\right)\right)\right]^p\right)\right]^{1/p}, \tag{72}$$

where $\bar{\alpha}_{sat} = \frac{N_c}{\pi}\alpha_{sat}, \bar{\alpha}_s(r^2) = \frac{N_c}{\pi}\alpha_s(r^2)$ and α_{sat} is fixed to 1. Parameters were fitted with $m_{uds} = 0.1\text{GeV}$, $m_c = 1.3\text{GeV}$ and $m_b = 4.5\text{GeV}$. The set from [30] Table 1 row 3 is taken with $\sigma_0 = 31,4055\text{mb}$, $Q_{s0}^2 = 0.4\text{GeV}^2$, $C = 2.586$ and $p = 0.807$. Variable number of flavours scheme has been used leading to $\Lambda_b = 88\text{MeV}$,$\Lambda_c = 120\text{MeV}$ and $\Lambda_{uds} = 144\text{MeV}$.

3.2 GBW

One of parametrizations is provided by the saturation model of Golec-Biernat and Wüsthöff (GBW)[32, 33]

$$\sigma_{q\bar{q}}(x,r) = \sigma_0\left(1 - e^{-\frac{r^2 Q_s^2(x)}{4}}\right) \qquad Q_s^2(x) = Q_0^2\left(\frac{x_0}{x}\right)^{\lambda}\ \text{GeV}^2 \tag{73}$$

$$Q_0^2 = 1\text{GeV}^2 \quad \sigma_0 = 23.03\text{mb} \quad x_0 = 0.0003 \quad \lambda = 0.288 \tag{74}$$

This dipole cross-section vanishes like r^2 at small distances, whereas it levels of at large distances exponentially. The saturation scale Q_s^2 is related to the gluon density in the transverse plane and the exponent λ determines the growth of the total and diffractive cross-sections with decreasing x. For dipole sizes larger than $1/Q_s$ the dipole cross-sections saturates at the level of σ_0. This parametrization comes from global fit to HERA data using three flavours with $m_f = 0.14\text{GeV}$.
More recent set of parameters was published by Kowalski-Motyka and Watt [1] Table 5.

$$Q_0^2 = 1\text{GeV}^2 \quad \sigma_0 = 23.9\text{mb} \quad x_0 = 0.000111 \quad \lambda = 0.287 \tag{75}$$

which includes also charm quark contribution with $m_c = 1.4\text{GeV}$ into the fit to HERA data in the range $0.25\text{GeV}^2 \leq Q^2 \leq 45\text{GeV}^2$. Note, that GBW parametrization accounts for one Pomeron exchange. As a consequence, the parametrization is accurate at high energies corresponding to $x \leq 0.01$. In addition to Pomeron part, Reggeon part can be added (and consequently add an interaction with valence quarks in the target). Nevertheless, the extraction of Reggeon part from data is not as accurate as Pomeron part, and so, the improvement of the prediction power is disputable[34].

3.3 KST

Another parametrization was published by Kopeliovich, Schäfer and Tarasov (KST)[35]

$$\sigma_{q\bar{q}}^N(s_q,r) = \sigma_0(s_q)\left(1 - e^{-\frac{r^2}{r_0^2(s_q)}}\right) \tag{76}$$

$$\sigma_0(s_q) = \sigma_{tot}^{\pi p}(s_q)\left(1 + \frac{3r_0^2(s_q)}{8\langle r_{ch}^2\rangle_\pi}\right) \tag{77}$$

$$r_0(s_q) = 0.88\left(\frac{s_q}{s_0}\right)^{-0.14}\text{fm} \qquad s_0 = 1000\text{GeV}^2 \tag{78}$$

$$\sigma_{tot}^{\pi p}(s_q) = 23.6\left(\frac{s_q}{s_0}\right)^{0.08}\text{mb} \qquad \langle r_{ch}^2\rangle_\pi = 0.44\text{fm}^2, \tag{79}$$

where all values depend on energy $s_q = sx_q$ rather than on Bjorken x and also an energy dependent parameter $\sigma_0(s_q)$ is introduced in order to correctly reproduce hadronic cross-sections. For the pion-proton total cross-section, the parametrization from [36] is used with fit parameters taken from [37]. This formula

also contains only Pomeron part of the dipole cross-section, nevertheless, the Reggeon part can be easily added by considering full form of the pion-proton cross-section(Barnett:1996hr)

$$\sigma_{tot}^{\pi p}(s_q) = 23.6 \left(\frac{s_q}{s_0}\right)^{0.08} + 1.425 \left(\frac{s_q}{s_0}\right)^{-0.45} \text{mb}. \tag{80}$$

3.4 IIM or CGC

This parametrization was proposed by Iancu, Itakura and Munier [38] including charm contribution

$$\begin{aligned}
\sigma_{q\bar{q}}(x,r,b) &= \sigma_0 N_0 \left(\frac{rQ_s(x)}{2}\right)^{2\gamma_{eff}(x,r)} & rQ_s(x) \leq 2 \\
&= \sigma_0 \left(1 - e^{-A\ln^2(BrQ_s(x))}\right) & rQ_s(x) > 2 \\
\gamma_{eff}(x,r) &= \gamma + \frac{1}{\kappa\lambda Y}\ln\left(\frac{2}{rQ_s(x)}\right) & Y = \ln\left(\frac{1}{x}\right),
\end{aligned} \tag{81}$$

where $\gamma_{eff}(x,r)$ is an effective anomalous dimension, $\kappa = 9.9$, $N_0 = 0.7$, $Q_s^2(x) = \left(\frac{x_0}{x}\right)^{\lambda}$ GeV ^{2} and $\sigma_0 = 2\pi R_p^2$. Parameters A and B are chosen to ensure continuity between both parts of the parametrization at $rQ_s(x) = 2$ as

$$\begin{aligned}
A &= -\frac{N_0^2\gamma^2}{(1-N_0)^2\ln(1-N_0)} \\
B &= \frac{1}{2}(1-N_0)^{-\frac{1-N_0}{N_0\gamma}}.
\end{aligned} \tag{82}$$

Parameters $, R_p, \gamma, x_0$ and λ has to be fitted to data. First fit from [1] keeps $\gamma = 0.63$ fixed and sets $\lambda = 0.177$, $x_0 = 0.0027 \times 10^{-4}$ and $\sigma_0 = 35.7$mb. The fit has been done with $m_f = 0.14$GeV for light quarks and $m_c = 1.4$GeV and data from H1 cover the range $0.25\text{GeV}^2 \leq Q^2 \leq 45\text{GeV}^2$. Alternative fit was performed in [39] with $\gamma = 0.7376$, $\lambda = 0.2197$, $x_0 = 0.1632 \times 10^{-4}$ and $\sigma_0 = 27.33$mb. The fit has been done with $m_f = 0.14$GeV for light quarks and $m_c = 1.4$GeV and data from H1 cover the range $0.25\text{GeV}^2 \leq Q^2 \leq 150\text{GeV}^2$. The most recent set of parameters comes from [40] and sets $\gamma = 0.762$, $\lambda = 0.2319$, $x_0 = 6.226 \times 10^{-4}$ and $\sigma_0 = 21.85$mb. The fit has been done with $m_f = 0.14$GeV for light quarks and $m_c = 1.27$GeV and data cover the range $0.25\text{GeV}^2 \leq Q^2 \leq 45\text{GeV}^2$.

3.5 IP-sat or b-Sat or BGBK

This parametrization coming from [16] is explicitly dependent on impact parameter b and, therefore, the dipole cross section does not need to be factorized.

$$\sigma_{q\bar{q}}(x,r,b) = \left(1 - e^{-\frac{\pi^2 r^2}{2N_c}\alpha_s(\mu^2)xg(x,\mu^2)T_g(b)}\right), \tag{83}$$

where $\mu^2 = \mu_0^2 + \frac{C}{r^2}$ is the scale of the gluon density, at which the gluon distribution function $xg(x,\mu^2)$ has to be evolved according to LO DGLAP without quarks

$$\frac{dg(x,Q^2)}{d\log Q^2} = \frac{\alpha_s}{2\pi}\int_x^1 \frac{dy}{y} g(y,Q) P_{gg}(x/y) \tag{84}$$

$$P_{gg}(x) = 6\left(\frac{x}{(1-x)_+} + \frac{1-x}{x} + x(1-x)\right) + \frac{27}{6}\delta(1-x), \tag{85}$$

where $[]_+$ is defined as

$$\int_x^1 dx f(x)\left[g(x)\right]_+ = \int_x^1 dx(f(x)-f(1))g(x). \tag{86}$$

The parameters C and μ_0 are fixed to $C = 4$ and $\mu_0^2 = 1.17$ and the profile function has a Gaussian form normalized to 1

$$T_g(b) = \frac{1}{2\pi B}\exp^{-\frac{b^2}{2B}}, \tag{87}$$

where $B = 4GeV^{-2}$. The initial gluon density for the DGLAP evolution was taken as

$$xg(x,\mu_0^2) = A_g x^{-\lambda_g}(1-x)^{5.6}. \tag{88}$$

The coupling constant is taken in a one-loop form for four flavours with $\Lambda_{QCD} = 0.156GeV$.

3.6 b-CGC

This parametrization was proposed by Kowalski, Motyka and Watt[1, 41] as a modification of the CGC parametrization

$$\begin{aligned}
\sigma_{q\bar{q}}(x,r,b) &= 2N_0\left(\frac{rQ_s(x,b)}{2}\right)^{2\gamma_{eff}(x,r,b)} && rQ_s(x,b) \leq 2 \\
&= 2\left(1 - e^{-A\ln^2(BrQ_s(x,b))}\right) && rQ_s(x,b) > 2 \\
\gamma_{eff}(x,r,b) &= \gamma + \frac{1}{\kappa\lambda Y}\ln\left(\frac{2}{rQ_s(x,b)}\right) && Y = \ln\left(\frac{1}{x}\right),
\end{aligned} \tag{89}$$

where $\gamma_{eff}(x,r,b)$ is an effective anomalous dimension, $\kappa = 9.9$, $Q_s^2(x,b) = \left(\frac{x_0}{x}\right)^\lambda\left(e^{-\frac{b^2}{2B_{CGC}}}\right)^{\frac{1}{\gamma}}$. Parameters A and B are chosen to ensure continuity between both parts of the parametrization at $rQ_s(x) = 2$ as

$$\begin{aligned}
A &= -\frac{N_0^2\gamma^2}{(1-N_0^2)^2\ln(1-N_0)} \\
B &= \frac{1}{2}(1-N_0)^{-\frac{1-N_0}{N_0\gamma}}.
\end{aligned} \tag{90}$$

Parameters $B_{CGC}, N_0, \gamma, x_0$ and λ has to be fitted to data. Original set of parameters come from [1] where $\gamma = 0.63$ is fixed and sets $N_0 = 0.417$, $\lambda = 0.159$, $x_0 = 5.95 \times 10^{-4}$ and $B_{CGC} = 5.5\text{GeV}^{-2}$. The fit has been done with $m_f = 0.14$GeV for light quarks and $m_c = 1.4$GeV and data from H1 cover the range $0.25\text{GeV}^2 \leq Q^2 \leq 45\text{GeV}^2$. This fit was later re-done on the same data in [41] by allowing γ to be a free parameter and sets $\gamma = 0.46$,$N_0 = 0.558$, $\lambda = 0.119$, $x_0 = 0.184 \times 10^{-5}$ and $B_{CGC} = 7.5\text{GeV}^{-2}$. The most recent set of parameters comes from [40] and sets $\gamma = 0.6492$,$N_0 = 0.3658$, $\lambda = 0.2023$, $x_0 = 0.00069$ and $B_{CGC} = 5.5\text{GeV}^{-2}$. The fit has been done with $m_f = 0.14$GeV for light quarks and $m_c = 1.4$GeV and data cover the range $0.75\text{GeV}^2 \leq Q^2 \leq 650\text{GeV}^2$.

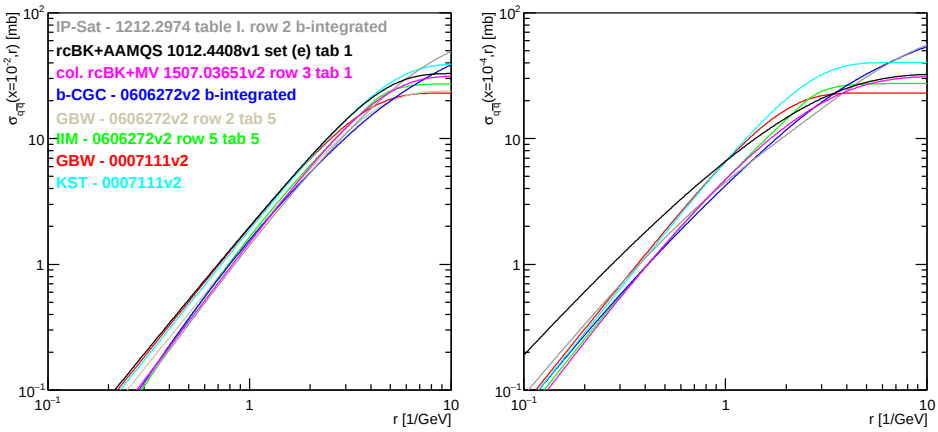

Figure 10: Comparison of integrated dipole cross-sections at fixed Bjorken x. Compare to Fig. 27 of [1].

References

[1] H. Kowalski, L. Motyka, and G. Watt, Phys.Rev. **D74**, 074016 (2006), arXiv:hep-ph/0606272.

[2] N. Armesto and A. H. Rezaeian, Phys.Rev. **D90**, 054003 (2014), arXiv:1402.4831.

[3] J. Berger and A. M. Stasto, JHEP **1301**, 001 (2013), arXiv:1205.2037.

[4] H. G. Dosch, T. Gousset, G. Kulzinger, and H. Pirner, Phys.Rev. **D55**, 2602 (1997), arXiv:hep-ph/9608203.

[5] G. P. Lepage and S. J. Brodsky, Phys.Rev. **D22**, 2157 (1980).

[6] J. Nemchik, N. N. Nikolaev, E. Predazzi, and B. Zakharov, Z.Phys. **C75**, 71 (1997), arXiv:hep-ph/9605231.

[7] J. Nemchik, N. N. Nikolaev, and B. Zakharov, Phys.Lett. **B341**, 228 (1994), arXiv:hep-ph/9405355.

[8] Particle Data Group, K. A. Olive *et al.*, Chin. Phys. **C38**, 090001 (2014).

[9] G. Sampaio dos Santos and M. V. T. Machado, J. Phys. **G42**, 105001 (2015), arXiv:1411.7918.

[10] S. J. Brodsky, T. Huang, and G. P. Lepage, The Hadronic Wave Function in Quantum Chromodynamics, 1980.

[11] J. R. Forshaw, R. Sandapen, and G. Shaw, Phys.Rev. **D69**, 094013 (2004), arXiv:hep-ph/0312172.

[12] L. Motyka and G. Watt, Phys. Rev. **D78**, 014023 (2008), arXiv:0805.2113.

[13] B. E. Cox, J. R. Forshaw, and R. Sandapen, JHEP **06**, 034 (2009), arXiv:0905.0102.

[14] J. Hufner, Yu. P. Ivanov, B. Z. Kopeliovich, and A. V. Tarasov, Phys. Rev. **D62**, 094022 (2000), arXiv:hep-ph/0007111.

[15] W. Lucha and F. F. Schoberl, Int. J. Mod. Phys. **C10**, 607 (1999), arXiv:hep-ph/9811453.

[16] H. Kowalski and D. Teaney, Phys. Rev. **D68**, 114005 (2003), arXiv:hep-ph/0304189.

[17] L. Frankfurt, W. Koepf, and M. Strikman, Phys. Rev. **D57**, 512 (1998), arXiv:hep-ph/9702216.

[18] E. Eichten, K. Gottfried, T. Kinoshita, K. D. Lane, and T.-M. Yan, Phys. Rev. **D17**, 3090 (1978), [Erratum: Phys. Rev.D21,313(1980)].

[19] E. Eichten, K. Gottfried, T. Kinoshita, K. D. Lane, and T.-M. Yan, Phys. Rev. **D21**, 203 (1980).

[20] C. Quigg and J. L. Rosner, Phys. Lett. **71B**, 153 (1977).

[21] A. Martin, Phys. Lett. **B93**, 338 (1980).

[22] W. Buchmuller and S. H. H. Tye, Phys. Rev. **D24**, 132 (1981).

[23] T. Lappi and H. Mantysaari, Phys. Rev. **C83**, 065202 (2011), arXiv:1011.1988.

[24] J. Cepila, J. G. Contreras, and J. D. Tapia Takaki, Phys. Lett. **B766**, 186 (2017), arXiv:1608.07559.

[25] J. L. Albacete and Y. V. Kovchegov, Phys.Rev. **D75**, 125021 (2007), arXiv:0704.0612.

[26] J. L. Albacete, N. Armesto, J. G. Milhano, and C. A. Salgado, Phys.Rev. **D80**, 034031 (2009), arXiv:0902.1112.

[27] J. L. Albacete, N. Armesto, J. G. Milhano, P. Quiroga-Arias, and C. A. Salgado, Eur.Phys.J. **C71**, 1705 (2011), arXiv:1012.4408.

[28] Y. V. Kovchegov and H. Weigert, Nucl.Phys. **A784**, 188 (2007), arXiv:hep-ph/0609090.

[29] I. Balitsky, Phys.Rev. **D75**, 014001 (2007), arXiv:hep-ph/0609105.

[30] E. Iancu, J. D. Madrigal, A. H. Mueller, G. Soyez, and D. N. Triantafyllopoulos, Phys. Lett. **B750**, 643 (2015), arXiv:1507.03651.

[31] L. D. McLerran and R. Venugopalan, Phys.Lett. **B424**, 15 (1998), arXiv:nucl-th/9705055.

[32] K. J. Golec-Biernat and M. Wusthoff, Phys.Rev. **D59**, 014017 (1998), arXiv:hep-ph/9807513.

[33] K. J. Golec-Biernat and M. Wusthoff, Phys.Rev. **D60**, 114023 (1999), arXiv:hep-ph/9903358.

[34] B. Kopeliovich, J. Raufeisen, A. Tarasov, and M. Johnson, Phys.Rev. **C67**, 014903 (2003), arXiv:hep-ph/0110221.

[35] B. Z. Kopeliovich, A. Schafer, and A. V. Tarasov, Phys.Rev. **D62**, 054022 (2000), arXiv:hep-ph/9908245.

[36] A. Donnachie and P. Landshoff, Phys.Lett. **B296**, 227 (1992), arXiv:hep-ph/9209205.

[37] Particle Data Group, R. M. Barnett *et al.*, Phys.Rev. **D54**, 1 (1996).

[38] E. Iancu, K. Itakura, and S. Munier, Phys. Lett. **B590**, 199 (2004), arXiv:hep-ph/0310338.

[39] G. Soyez, Phys. Lett. **B655**, 32 (2007), arXiv:0705.3672.

[40] A. H. Rezaeian and I. Schmidt, Phys. Rev. **D88**, 074016 (2013), arXiv:1307.0825.

[41] G. Watt and H. Kowalski, Phys. Rev. **D78**, 014016 (2008), arXiv:0712.2670.